Home   Search   Collections   Journals   About   Contact us   My IOPscience

Plasma wave oscillations in nanometer field effect transistors for terahertz detection and emission

Plasma wave oscillations in nanometer field effect transistors for terahertz detection and emission

W Knap[1,2]**, F Teppe**[2]**, N Dyakonova**[2]**, D Coquillat**[2] **and J Łusakowski**[3]

[1] RIEC, Ultra-broadband Signal Processing, Tohoku University, 2-1-1 Katahira,
Aoba-ku, 980-8577, Japan
[2] Université Montpellier2 and CNRS–GES–UMR5650, Place E Bataillon,
34095 Montpellier, France
[3] Institute of Experimental Physics, University of Warsaw, Hoza 69 Warsaw, Poland

E-mail: knap.wojciech@gmail.com

Abstract
The channel of a field effect transistor can act as a resonator for plasma waves propagating in a two-dimensional electron gas. The plasma frequency increases with reduction of the channel length and can reach the terahertz (THz) range for nanometer size transistors. Recent experimental results show these transistors can be potential candidates for a new class of THz detectors and emitters. This work gives an overview of our recent relevant experimental results. We also outline unresolved problems and questions concerning THz detection and emission by nanometer transistors.

1. Introduction

The channel of the field effect transistor (FET) with well defined dimensions can act as a resonator for plasma waves propagating in a two-dimensional (2D) electron gas. The plasma frequency of this resonator depends on its dimensions and for gate lengths of nanometer size and typical carrier densities this can reach the terahertz (THz) range. As predicted in [1] a steady current flow through a FET can become unstable with the generation of plasma waves, which leads to the emission of electromagnetic radiation at the plasma wave frequency. The nonlinear properties of the 2D plasma in the transistor channel can also be used for a resonant and voltage tunable detection of THz radiation [2].

In this work we present an overview of our recent results on THz emission and detection obtained in different types of GaInAs/GaAs, InGaAs/InP and AlGaN/GaN nanometer high electron mobility FETs (HEMTs) [3–10]. We show that (i) the experimental emission and detection frequencies correspond roughly to the calculated characteristic plasma wave frequencies, and (ii) the emission appears once the drain current exceeds a certain well defined threshold value—as predicted by the instability model [1]. We also present and discuss many experimental observations that remain unexplained or are difficult to interpret on the basis of existing theories.

The first experimental results were obtained at cryogenic temperatures [3, 4, 6]; however, it has been recently shown that GaAs/AlGaAs and InGaAs/InP HEMTs can operate as detectors at room temperature [7, 9]. Also, Si metal-oxide-semiconductor FETs (MOSFETs) with gate lengths of 120–300 nm have been demonstrated to be efficient room temperature detectors of sub-THz electromagnetic radiation [10]. Independently, the first room temperature THz emission from a 150 nm gate length GaN/AlGaN transistor was observed [5]. Therefore, except for evident interest in the basic physics of plasma excitations in nanometer systems, studying these excitations in nanometer FETs is important for emerging applications.

The paper is organized as follows: section 2 describes the main results in detection and section 3 reports the key experiments in THz emission.

2. Terahertz detection

The mechanism of detection is usually described by the theory of Dyakonov and Shur (D–S) which concerns plasma waves in the 2D electron gas confined in the transistor channel [1, 2].
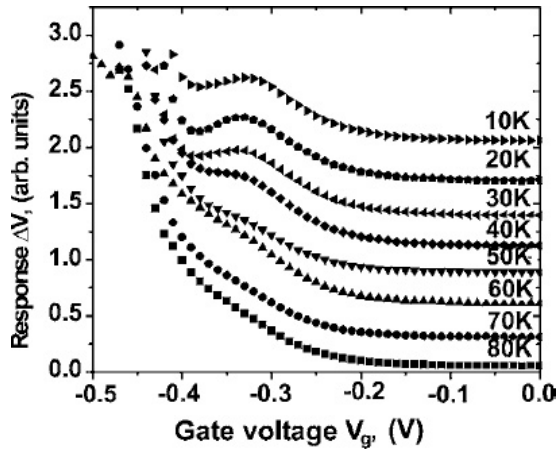
Figure 1. Response of InGaAs/InAlAs-based HEMT exposed to 2.5 THz radiation as a function of the gate voltage at different temperatures. A resonant plasma detection signal develops at low temperatures. For clarity, curves are vertically shifted. Reprinted with permission from [8]. Copyright 2006, American Institute of Physics.

Figure 2. Response of InGaAs/InAlAs-based HEMT to THz radiation, as a function of the gate voltage at different (1.8, 2.5, and 3.1 THz) frequencies and at $T = 10$ K. The curves are vertically shifted for clarity. Dashed lines indicate the zero response level. The calculated plasmon frequency as a function of the gate voltage for $U_{th} = -0.41$ V is shown by the solid line (left axis). The error bars correspond to the linewidth of the measured plasmon resonance peaks. Reprinted with permission from [8]. Copyright 2006, American Institute of Physics.

Using this model, one can show that the detection process leads to rectification of the THz wave and development of a constant source to drain voltage, ΔU. The value of this voltage depends on the carrier density in the channel which may be controlled by the gate voltage value, U_g.

In spite of a well developed theoretical basis and first experimental observations, many aspects of the physical mechanism of such detection are still not well understood. Two basic open questions are: (i) what is the main plasma resonance broadening/damping mechanism, and (ii) how does the incident radiation of wavelength λ couple to the transistor of typical dimensions much smaller than λ.

The first detection experiments showing a resonant plasma detection tuned with the carrier density in the channel of submicron GaInAs/GaAs HEMTs were performed at 0.6 THz [6]. Subsequently high mobility InGaAs/InAlAs transistors in the spectral range 1.8–3.1 THz were studied [8]. In the majority of experiments the incoming radiation is a monochromatic beam generated by either a Gunn diode, a backward wave oscillator (BWO) or a CO_2 pumped molecular THz laser. In detection experiments the gate voltage is tuned to control the carrier density under the gate (the gated part of the channel), which allows the resonant plasma frequency to be swept through the frequency of incident radiation. Figure 1 shows an example of a resonant plasma detection at 2.5 THz. At higher temperatures (above 80 K), the signal typically does not reveal any resonance. The response voltage increases monotonically as the gate polarization approaches the threshold voltage. However, with decreasing temperature, the response develops an additional resonant maximum.

The response at a constant temperature of 10 K and at excitation frequencies of 1.8, 2.5, and 3.1 THz is shown in figure 2. A continuous line in figure 2 shows the theoretical dependence of the plasma frequency as a function of the gate voltage. Figure 2 shows that as the excitation frequency shifts from 1.8 to 3.1 THz, the plasma resonance frequency
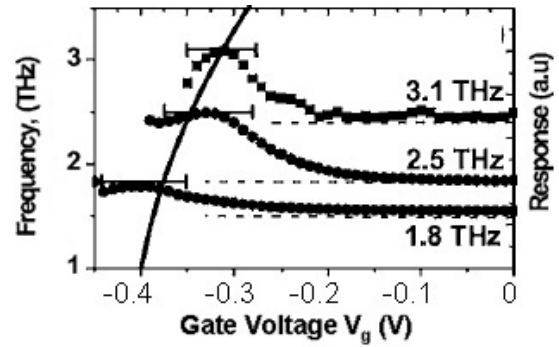
moves with the gate voltage in approximate agreement with theoretical predictions. The theory gives the correct order of magnitude of the frequency and a correct trend as a function of the gate voltage. However, the resonance is much broader than theoretically expected.

The most convenient way to present this problem is to consider the so-called quality factor Q. From the experimental point of view, Q is an important quantity because it describes the ratio of the resonant line position (in frequency or voltage) with respect to the linewidth. Theoretically, the quality factor can be written as $Q = \omega\tau$, where $\omega = 2\pi f$ is the excitation frequency and τ denotes the electron momentum relaxation time [1, 2]. The inverse of τ corresponds to the plasma resonance linewidth in terms of frequency.

For $\omega\tau \ll 1$, the plasma oscillations are expected to be overdamped; consequently, the response is expected to show a nonresonant, monotonic behavior. In the opposite case, when the quality factor becomes much larger than 1, narrow plasma resonance peaks are expected. The main motivation behind changing the transistor material system from GaInAs/GaAs—as used in first experiments [3, 6]—to InGaAs/InP [8] and using higher excitation frequencies (up 3 THz instead of 0.6 THz) was to improve the quality factor.

The greater carrier lifetime (the mobility) combined with the use of higher excitation frequencies was expected to result in an increase of the quality factor by at least one order of magnitude and the observation of sharp plasma resonances. However, the experimentally observed plasma resonances remained broad even using a 3 THz excitation—with a quality factor $\sim$2–3. The physical origin of an additional line broadening remains unclear. Understanding the origin of the broadening and minimizing it is one of the most important experimental and theoretical challenges.

Two main hypotheses regarding the origin of the additional broadening are currently under consideration: (i) the existence of oblique plasmon modes [11] and (ii) an additional damping due to the leakage of gated plasmons to ungated
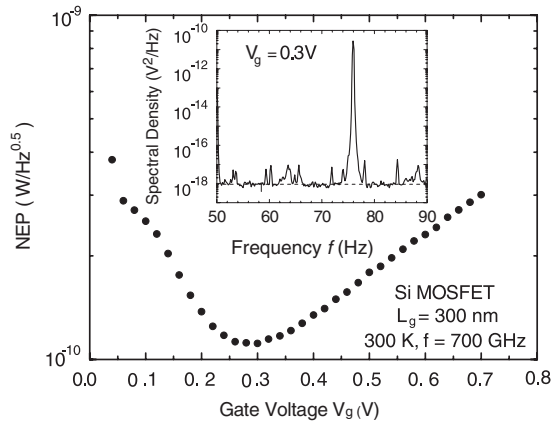
Figure 3. Noise equivalent power as a function of the gate voltage for Si MOSFETs with a 300 nm gate length, $T = 300$ K. The inset shows the spectral density including the detected signal and the background noise for the transistor with $L_g = 300$ nm. $V_g = 0.3$ V. Reprinted with permission from [10]. Copyright 2006, American Institute of Physics.

Figure 4. Detection signal as a function of the angle between the direction of the polarization vector and a symmetry axis of the transistor (the latter coincides with the horizontal line in the plot) for a GaAs/GaAlAs Fujitsu HEMT. Adapted from [15].

transistor regions [12]. The first hypothesis is related to the fact that in realistic devices the gate width is much greater than the gate length. Thus, the transistor channel serves as a waveguide rather than a resonator for plasma waves. In such a case the plasma waves can propagate not only in the source–drain direction but also in the oblique directions. The spectrum of plasma waves in this case is continuous and limited to a lower frequency defined by the resonant plasma frequency corresponding to waves propagating in the source–drain direction. This model and its consequences have been recently addressed in [11] and will be discussed in more detail in the next section in relation to the THz emission experiments.

The second hypothesis, a leakage of gated plasmons to ungated regions of the channel [12], is related to the observation that in the channel of a HEMT the gate covers only a small part of the source–drain distance. Therefore, the plasma under the gate region cannot be treated independently of the plasma in the ungated parts. An interaction between the two plasma regions can lead not only to a modification of the resonant frequency—as considered in [13]—but also to a line broadening. Popov *et al* [12] have recently calculated the THz absorption spectrum of an HEMT with a short recessed gate and shown that the main contribution to the linewidth of the gated plasmon resonance comes from an intermode plasmon–plasmon scattering. They found that the intermode plasmon–plasmon scattering may play a role in the main plasmon damping mechanisms.

Even if the problem of the broadening of the plasma resonances is still unclear, plasma oscillations in nanotransistors are very promising for THz detection applications. This can be illustrated by experiments on nonresonant detection in Si MOSFETs [10]. The results presented in figure 3 show the noise equivalent power (NEP) measured at room temperature at 0.7 THz. One can see that the value of NEP is comparable with the best current commercial room temperature THz detectors. It should be stressed at this point that transistors used
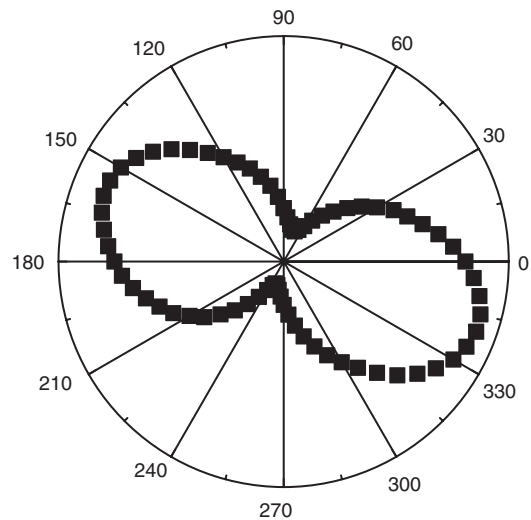
in these measurements were not fitted with any special antennas or lenses. The radiation was coupled only by the bonding wires and the metal pads of the transistor electrodes. From the point of view of future applications it is important to consider the optimization of the radiation–detector coupling.

The problem of radiation coupling and angular response has been recently addressed by Sakowicz *et al* [14, 15]. In recent experiments they have found that for relatively low sub-THz frequencies of the order of 100 GHz, the radiation couples to the transistor via an antenna formed mainly by the bonding wires [14]. For frequencies above 200 GHz, the metal pads of the source, drain, and gate electrodes play the role of an antenna and the THz radiation coupling efficiency is strongly related to the layout of these contact electrodes [14, 15]. For transistors whose electrode layout meant unequal source–gate and drain–gate capacitances, a clear angular dependence of a device response was observed with respect to the direction of the linearly polarized electric field of the incoming radiation. This is illustrated in figure 4 in which a typical '8'-like shape means that a preferential polarization direction exists.

In the polarization experiments, a linearly polarized radiation illuminated the transistors at normal incidence. The detection signal was registered as a function of the angle, α, between the direction of the polarization vector and a symmetry axis of the transistor. The results are shown in polar coordinates in figure 4. The shape of the observed dependence can be approximated by $\cos^2 \alpha$. This indicates that the response of the transistor chip can be modeled as resulting from the excitation of a linear dipole.

Results shown in figure 4 were obtained for a commercially available Fujitsu HEMT with a gate length of 150 nm and the radiation used was generated by a 100 GHz Gunn diode. The symmetry line of the experimental data in figure 4 does not coincide with any of the two symmetry axis of the transistor (the horizontal and vertical lines in the plot in figure 4). Numerical simulations showed that at 100 GHz
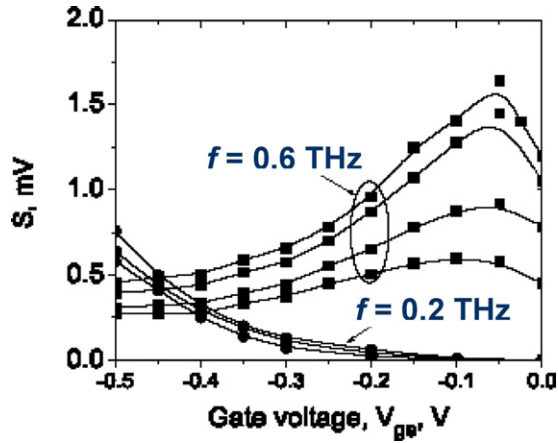
Figure 5. Detection signal as a function of gate bias for 600 and 200 GHz sources for different drain–source voltages: at 600 GHz, drain voltages from the bottom to the top: 400, 500, 750 mV, and 1 V; at 200, drain voltages from the bottom to the top: 250, 500 mV, and 1 V. Adapted from [9].
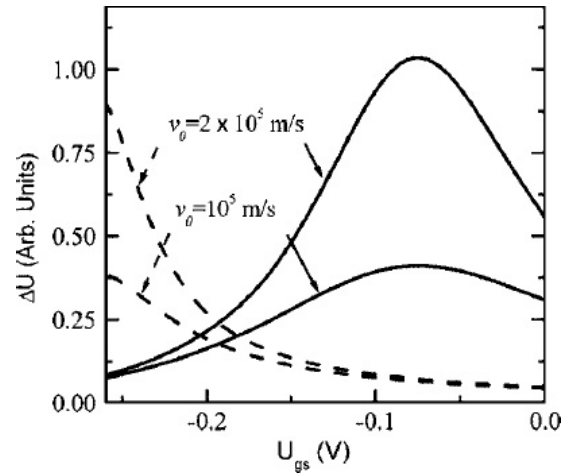

Figure 6. Calculations of the photoconductivity signal according to equation (1) for the frequencies 200 GHz (dashed lines) and 600 GHz solid lines. Reprinted with permission from [7]. Copyright 2005, American Institute of Physics.

the bonding wires to the metallic pads of the source, drain and gate would play the biggest role in coupling the transistor chip with the external radiation. In other words, at this frequency, the orientation of the excited dipole is defined by the spacial arrangement of the bonding wires.

A significant improvement in sensitivity can be obtained by applying a drain current to the transistor. The influence of the current on the resonant detection was demonstrated using a 250 nm gate length commercial GaAs HEMT and 200 and 600 GHz sources [9]. Nonresonant detection changed to resonant detection when the transistor was driven into the saturation region. The photoconductive response versus the gate voltage for 600 and 200 GHz is shown in figure 5. For the 200 GHz source, only typical nonresonant signals were observed even for large values of current. For a 600 GHz source, after an initial increase of the nonresonant background signal with applied drain voltage/current, the resonant structure appears at higher drain bias.

The results suggest that the drain current affects the plasma relaxation rate and the quality factor. As mentioned above, when the quality factor $\omega_0\tau \ll 1$ (τ is the relaxation time), the response is a monotonic function of ω and the gate voltage (a nonresonant broadband detection). For $\omega_0\tau \gg 1$, the FET operates as a resonant detector. In this case, the response is given by [16]:

$$\Delta U \propto \frac{1}{(\omega - \omega_0)^2 + \left(\frac{1}{2\tau}\right)^2}. \tag{1}$$

Previously, the effect of I_d on detector response was studied by Lü and Shur in the nonresonant regime [17]. They showed that the increase of I_d leads to a dramatic increase of the nonresonant THz detection responsivity. This increase was explained by an increase in the asymmetry of the source–gate and drain–gate capacitances with higher drain bias. To interpret our results, we use a theory developed in [7], where it was shown that the resonance response for $I_d \neq 0$ is given by

equation (1) with the replacement $\tau \rightarrow \tau_{eff}$. Here, $1/\tau_{eff}$ is the effective linewidth given by:

$$1/\tau_{eff} = 1/\tau + 2v_0/L \tag{2}$$

where v_0 is the electron drift velocity. With the increase of the current, the electron drift velocity increases, leading to the increase in τ_{eff}. This corresponds to the increase of the quality factor. When $\omega_0\tau_{eff}$ approaches unity, the detection becomes resonant.

Figure 6 shows the response calculated from equation (1) for drift velocities of 1×10^5 and 2×10^5 m s^{-1}. The relaxation time taken, $\tau = 0.34$ ps, corresponded to the optical phonon scattering time. One can see a qualitative agreement between the calculations and experimental observations. The response at 200 GHz has a nonresonant character even for the highest drift velocity values. For 600 GHz, the resonance becomes visible as the effective drift velocity is increased. It should be stressed that applying current allows the observation of *room temperature* resonant detection of the 0.6 THz radiation.

Recently, the first applications of nanotransistors for THz imaging were reported. The plasma wave nanometer transistors were shown to have sufficient speed and sensitivity for this application. Imaging with a GaAs/AlGaAs HEMT acting as a single pixel operating at room temperature was demonstrated at a frequency of 0.6 THz [18]. A focused beam scanned the Croix du Languedoc, concealed in a paper envelope and attached to xy linear motor stages (figure 7). The power of the incident beam on the Croix was 90 μW, the spot radius was 700 μm, and the response of the transistor was measured using a lock-in amplifier with an integration time of 10 ms. For comparison, a detector array operating at video rates would require a pixel element with 30 ms response time. Thus, this data suggest that a plasma wave nanotransistor array could be an excellent solution for a real time THz camera.
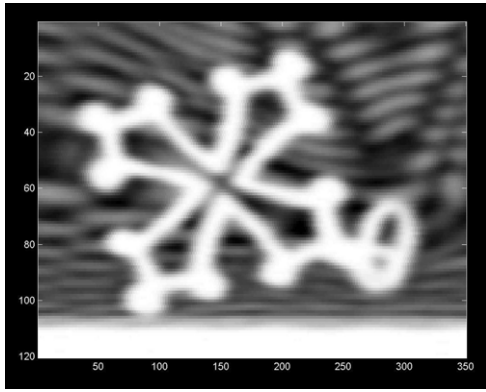
Figure 7. THz transmission image of the Croix du Languedoc hidden in a paper envelope with a GaAs/AlGaAs HEMT used as a single pixel and operated at 300 K. Axis scale is in millimeters, and the linear intensity is given in relative units. The image consists of 190×1960 pixels and was taken in 7 min (10 ms/pixel). The interference pattern in the background is caused by multiple reflections between the envelope sheets.

3. Emission

Theoretical predictions that the current-carrying state of a FET may become unstable, leading to the spontaneous generation of plasma waves in the transistor channel [1, 2], have lead to intense experimental studies [3–10]. Experimental investigation of THz emission from nanotransistors was performed with two experimental systems: a cyclotron resonance spectrometer [3, 19] and a Fourier transform spectrometer equipped with an ultra-sensitive bolometer [5]. The cyclotron resonance spectrometer was used earlier to investigate a weak THz cyclotron resonance emission in GaAs/AlGaAs heterojunctions [20]. In this spectrometer, the THz source and detector under study are placed in a copper waveguide, cooled to 4.2 K and completely isolated from 300 K background radiation. The emitted radiation is analyzed by a magnetically tunable InSb cyclotron detector calibrated with InSb and GaAs bulk emitters. The emission frequency can be tuned by the magnetic field in a wide range from sub-THz up to a few THz.

In the emission experiments, lattice-matched nanometer gate length InGaAs/AlInAs HEMTs were used. The gate length was 60 nm, and the drain–source separation was 1.3 μm. An InP-based HEMT was chosen for its high InGaAs channel mobility and high sheet carrier density. Voltage pulses were applied between drain and source, and a standard lock-in technique was used to detect the emitted signal. A few measured spectra are shown in figure 8. The spectra exhibit one main emission line. The peak emission frequency shifts from 0.42 to 1 THz with increasing the source–drain voltage. We would like to stress that no emission was observed until the drain current/drain voltage reached a certain threshold. Above the threshold, a strong emission signal, which increased sharply with applied bias, was observed. This threshold-like behavior is the main argument used in interpreting the observed emission as due to plasma instability. This threshold-like behavior was very well documented in [5].
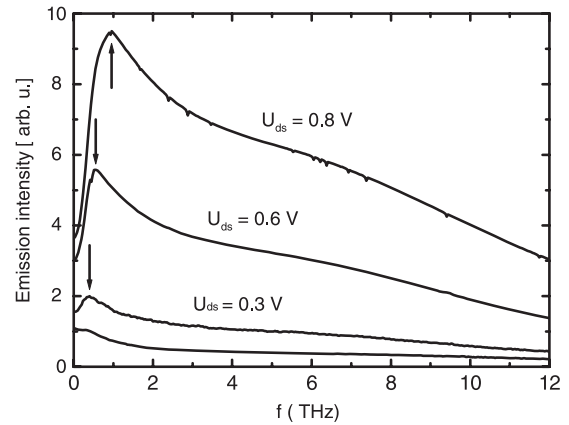

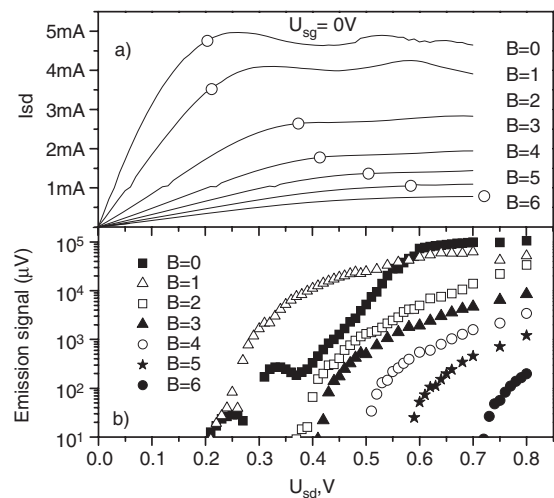**Figure 8.** Emission spectra of InGaAs/InP HEMT. Adapted from [3].

Figure 9. (a) Current–voltage characteristics for an InGaAs/AlInAs HEMT with a magnetic field in the range from 0 to 6 T and zero gate polarization. The open points on the curves mark the threshold of THz emission U_{th}. (b) Emission intensity as a function of the source–drain bias under magnetic field in the range from 0 to 6 T. Adapted from [5].

The threshold behavior can be clearly seen in figure 9 showing the resonant line emission intensity versus source–drain voltage. The threshold voltage increases with applied magnetic field due to magnetoresistance effects [5]. The observed radiation power was in the nW range as compared to the pW power of the bulk InSb emitters used for calibration [3].

The first THz emission experiments were performed at cryogenic temperatures. However, THz emission from nanotransistors persists up to room temperature. This is illustrated in figure 10. One can see the similarity with the 4.2 K experiments: THz emission at 300 K appears when the source–drain voltage/current reaches a threshold value. Figure 10 also shows the output characteristics (drain current as a function of the drain–source bias). A comparison of the emission intensity and the drain current illustrates the fact that the emission is observed under conditions of saturation of the transistor. It is also worth noting that the emission usually begins close to the region where the output characteristics show
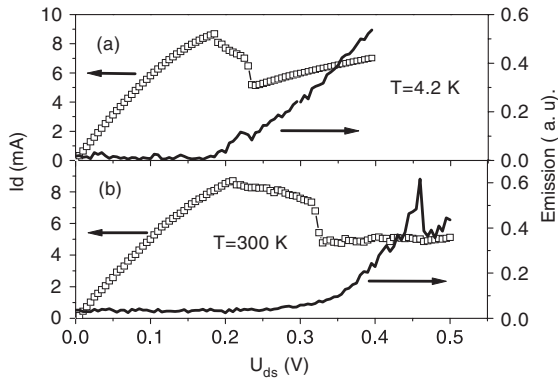
Figure 10. Current–voltage characteristics and emission intensities for an InAlAs/InGaAs HEMT at 4.2 K, $U_{gs} = 0$ (a) and 300 K, $U_{gs} = 0.025$ V (b). Reprinted with permission from [5]. Copyright 2006, American Institute of Physics.
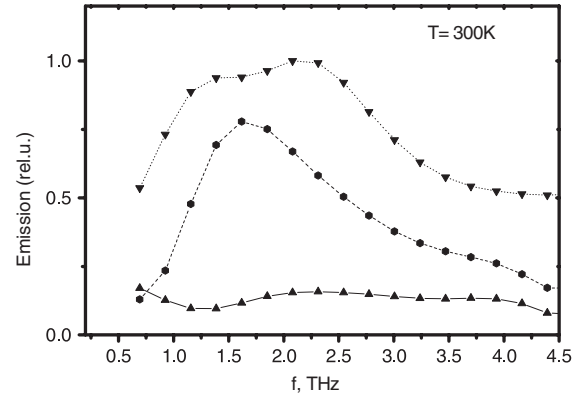

Figure 11. Emission spectra at 300 K for AlGaN/GaN HEMT at $U_{ds} = 8$ V, ▲—$U_{gs} = 0$, ●—$U_{gs} = -1.1$ V, ▼—$U_{gs} = -4$ V. Reprinted with permission from [5]. Copyright 2006, American Institute of Physics.

a strong instability, indicated by a step-like decrease of the drain current. At present, the relation between the emission and this instability is not clear. It is probable that the onset of THz emission is responsible for this behavior.

Room temperature THz emission was also observed from other HEMTs. A GaN/AlGaN HEMT appeared to be the most promising device, showing a room temperature emission strong enough to be analyzed with a Fourier transform spectrometer [5]. Emission spectra for a few values of the gate voltage are shown in figure 11. One can see that for gate polarizations $U_g = 0$ V and $U_g = -1$ V a broadband emission in the region between 1 and 3 THz can be observed. The threshold voltage of this transistor was close to $U_g = -4$ V. One can see that for this gate polarization THz emission disappears and only background level radiation is registered.

It is also very probable that depending on the source–drain polarization the mechanism of THz generation changes. This is illustrated in figure 12. In the upper panel the $I(V)$ characteristic and integrated radiation intensity versus drain voltage are plotted. In the lower panel one can see an example of two spectra measured using an InSb detector at $U_{sd} = 3$ and 4 V. It is evident that although the integrated THz intensities for these two polarizations are similar, the spectra have a very different character.

The experimental results indeed demonstrate that THz emission appears when the drain current exceeds a certain threshold value. Also, the radiation frequencies are in a reasonable agreement with estimates for fundamental plasma modes [3, 7]. However, some other features predicted in [1] such as a strong dependence of the radiation frequency on the gate dimension and gate bias have yet to be observed. Therefore, the existing experimental results do not allow us to establish unambiguously whether the observed emission is indeed related to the instability predicted in [1].

It should be noted that the analytical theory and experimental results are difficult to compare directly for two main reasons: (i) the theory concerns only the linear region of the current–voltage dependence, while most of the experimental observations are possible only when the transistor is driven into the saturation regime and (ii) the experimental
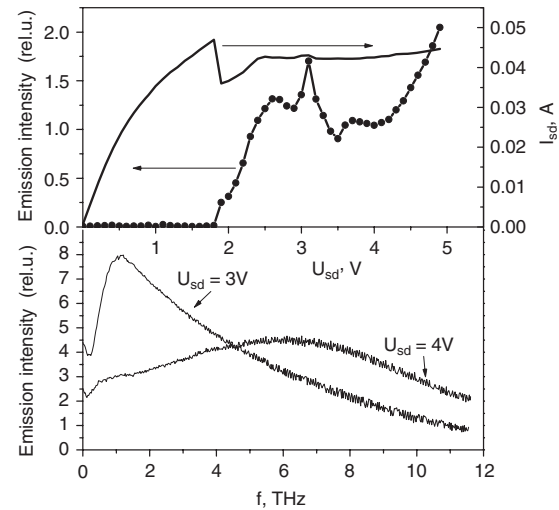

Figure 12. Current–voltage characteristic and the emission intensity for AlGaN/GaN HEMT at 4.2 K, $U_g = -1$ V (upper figure). Emission spectra at 4.2 K for the same sample, $U_g = -1$ V (lower figure).

geometry is very different from the one-dimensional model adopted in [1].

In fact, the theory in [1] considers a transistor with the gate width much smaller than the length. Experiments were carried out, however, for transistors with the width of the gate much larger than its length. The plasma wave instabilities for this case have been only recently considered [11]. It has been shown that under such conditions the one-dimensional model is not appropriate, since oblique plasma waves with a nonzero component of the wave vector in the direction perpendicular to the source–drain axes can propagate. In this realistic geometry, another type of instability can be excited in addition to that predicted in [1]. This new type of instability corresponds to plasma waves generated at the gate border and traveling in the direction perpendicular to the current. This instability should lead to relatively wide spectra and can explain, at least partially, the observed broadband emission spectra [11].

Furthermore, strong heating of electrons may lead to a real space transfer and to population of higher valleys. This

could result in a negative differential resistance, which could in principle persist up to THz frequencies. Some possible mechanisms leading to ultra-fast Gunn type oscillation were recently predicted based on Monte Carlo simulations [21, 22].

Another possibility to explain this broadband background emission is hot plasmon emission. Effectively, the incoherent hot plasmon waves can be excited in the channel by hot electrons. This phenomenon is well known, especially in grating structures [23, 24] but can also be important in a single transistor in which the metal pads play the role of coupling antenna/grating.

4. Conclusions

Recent experimental results show that nanometer transistors can be potential candidates for a new class of THz detectors and emitters. These properties are related to the fact that the channel of a high electron mobility transistor can act as a resonator for plasma waves propagating in a 2D electron gas. We have shown that THz emission and detection by nanometer size FETs persists from 4.2 K up to room temperature. The exact physical mechanisms responsible for the plasma resonance broadening and the origin of the observed emission are yet to be clarified. However, experimental results demonstrate the possibility of miniature THz sources based on nanotransistors. Also nanotransistor-based detectors have already been shown to be operational for THz imaging applications.

Acknowledgments

References

[1] Dyakonov M and Shur M S 1993 *Phys. Rev. Lett.* **71** 2465
[2] Dyakonov M I and Shur M S 1996 *IEEE Trans. Electron. Devices* **43** 380
[3] Knap W, Łusakowski J, Parenty T, Bollaert S, Capy A, Popov V V and Shur M S 2004 *Appl. Phys. Lett.* **84** 3523
[4] Dyakonova N, Teppe F, Łusakowski J, Knap W, Levinshtein M, Bollaert S and Cappy A 2005 *J. Appl. Phys.* **97** 114313
[5] Dyakonova N, El Fatimy A, Łusakowski J, Knap W, Dyakonov M I, Poisson M A, Morvan E, Bollaert S, Shchepetov A, Roelens Y, Gaquiere Ch, Theron D and Cappy A 2006 *Appl. Phys. Lett.* **88** 141906
[6] Knap W, Deng Y, Rumyantsev S and Shur M S 2002 *Appl. Phys. Lett.* **81** 4637
[7] Teppe F, Veksler D, Kachorovski V Yu, Dmitriev A P, Rumyantsev S, Knap W and Shur M S 2005 *Appl. Phys. Lett.* **87** 052107
[8] El Fatimy A, Teppe F, Dyakonova N, Knap W, Seliuta D, Valušis G, Shchepetov A, Roelens Y, Bollaert S, Cappy A and Rumyantsev S 2006 *Appl. Phys. Lett.* **89** 131926
[9] Teppe F, Orlov M, El Fatimy A, Tiberj A, Knap W, Torres J, Gavrilenko V, Shchepetov A, Roelens Y and Bollaert S 2006 *Appl. Phys. Lett.* **89** 222109
[10] Tauk R, Teppe F, Boubanga S, Coquillat D, Knap W, Meziani Y M, Gallon C, Boeuf F, Skotnicki T, Fenouillet-Beranger C, Maude D K, Rumyantsev S and Shur M S 2006 *Appl. Phys. Lett.* **89** 253511
[11] Dyakonov M I 2008 *Semicond. Sci. Technol.* at press
[12] Popov V V *et al* 2008 *Appl. Phys. Lett.* at press
[13] Ryzhii V, Satou A, Knap W and Shur M S 2006 *J. Appl. Phys.* **99** 084507
[14] Sakowicz M, Łusakowski J, Karpierz K, Grynberg M, Kohler K, Valusis G, Gołaszwska K, Kamińska E and Piotrowska A 2008 *Appl. Phys. Lett.* **92** 203509
[15] Sakowicz M, Łusakowski J, Karpierz K, Grynberg M and Gwarek W 2008 at press
[16] Veksler D, Teppe F, Dmitriev A P, Kachorovskii V Yu, Knap W and Shur M S 2006 *Phys. Rev.* B **73** 12
[17] Lü J Q and Shur M S 2001 *Appl. Phys. Lett.* **78** 2587
[18] Lisauskas A, von Spiegel W, Boubanga-Tombet S, El Fatimy A, Coquillat D, Teppe F, Dyakonova N, Knap W and Roskos H G 2008 *Electron. Lett.* **44** 408
[19] Knap W, Dur D, Raymond A, Meny C, Leotin J, Huant S and Etienne B 1992 *Rev. Sci. Instrum.* **63** 3293
[20] Chaubet C, Raymond A, Knap W, Mulot J Y, Baj M and André J P 1991 *Semicond. Sci. Technol.* **6** 160
[21] Mateos J, Perez S, Pardo D and Gonzalez T 2006 *International Conf. on Indium Phosphide and Related Materials Conf. Proc.* p 313
[22] Perez S, Gonzalez T, Pardo D and Mateos J 2008 *J. Appl. Phys.* **103** 094516
[23] Höpfel R A, Vass E and Gornik E 1982 *Phys. Rev. Lett.* **49** 1667
[24] Meziani Y M, Handa H, Knap W, Otsuji T, Sano E, Popov V V, Tsymbalov G M, Coquillat D and Teppe F 2008 *Appl. Phys. Lett.* at press